

Studies of thermal annealing and optical transmission of PET plastic for applications in superstrate-oriented thin film silicon solar cells

M. Z. PAKHURUDDIN*, K. IBRAHIM, A. ABDUL AZIZ

Nano-Optoelectronics Research and Technology Laboratory, School of Physics, Universiti Sains Malaysia, 11800 Minden, Penang, Malaysia

This paper studies relationship between thermal annealing and optical transmission of polyethylene terephthalate (PET) for applications in superstrate-oriented in thin film silicon solar cells. Differential scanning calorimetry (DSC) reveals that the original PET sample is semi-crystalline in nature with crystallinity (X_c) of 25.094%. Plot of enthalpy of fusion (ΔH_f) and X_c of samples with increased annealing temperature ($t = 60$ min) illustrates that both parameters increase almost linearly with increased annealing temperature. Optical transmission measurement shows that the original PET has a very high transmission (around 85%) in the visible and infra-red (IR) region, making it suitable as a superstrate material in thin film silicon solar cells. However, transmission decreases with increased temperature and is believed to be due to scattering effects of the incident light by various sizes of growing crystallites within the annealed samples. Correlation plot between optical transmission and X_c of the annealed samples shows that as X_c increases, the optical transmission reduces gradually until a sharp reduction at X_c of more than 28% (i.e. at temperature $\geq 180^\circ\text{C}$). These effects are very critical in the fabrication of thin film silicon solar cells in superstrate orientation but pose no issues for substrate orientation.

(Received June 25, 2014; accepted September 11, 2014)

Keywords: Polyethylene terephthalate, Crystallinity, Transmission, Thin film silicon solar cells

1. Introduction

Polyethylene terephthalate (PET) is an excellent polymeric material that has attracted interests of many parties in photovoltaics (PV) due to its low-cost, flexibility, light-weight, moderate temperature resistance and high optical transmission (80 - 90% in visible region)

[1, 2]. Due to these properties, PET has found wide applications in the fabrication of thin film solar cells and thin film transistors for display technologies [3]. Besides, using flexible substrate like PET leads to possibility for low-cost roll-to-roll deposition technique which is way cheaper than the current vacuum-based depositions [4].

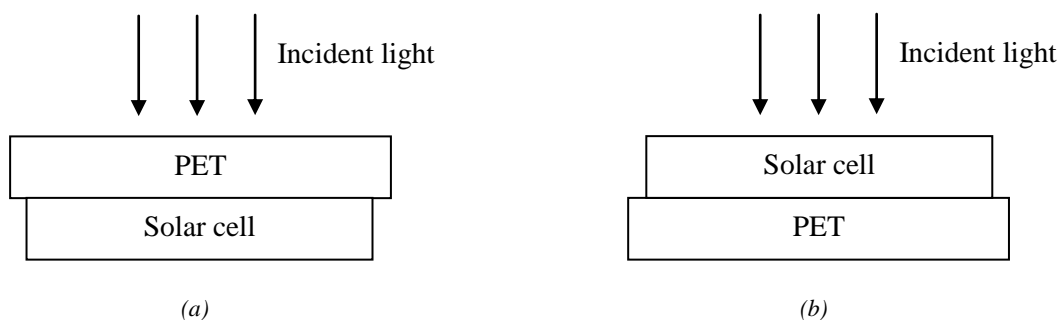


Fig. 1. Schematic representation of (a) superstrate (b) substrate-oriented thin film solar cells (not to scale).

Thermal annealing is a very important process step in thin film silicon solar cells fabrication. It is normally employed to suppress defects density introduced during film deposition while improving crystallinity and grain size of the absorber layers in order to maximise solar cells performance [5]. Optimising annealing process is very crucial for applications of PET plastic in thin film silicon

solar cells in superstrate orientation (as illustrated in Fig. 1 (a), Fig. 1 (b) refers to substrate orientation) because the PET has to allow maximum incident light to pass through it to the solar cell absorber layer to generate maximum photocurrent even though after getting through annealing process during cells fabrication [6]. Therefore, it is very important to know the optimum annealing parameters so

that unwanted reduction in PET optical transmission that could severely affect the output current and conversion efficiency of the cells can be avoided during the whole fabrication processes.

This paper aims to investigate relationship between thermal annealing and optical transmission of PET plastic for applications in superstrate-oriented thin film silicon solar cells. After thermal annealing, thermal and optical properties of the samples are analysed. Correlations between these parameters are established and effects towards its applications in thin film silicon solar cells in superstrate orientation are discussed.

2. Experimental

In this experiment, PET of 250 μm thickness from Penfibre Sdn. Bhd. (Film Division, Malaysia) is used. The PET samples are firstly cleaned in Decon 90 chemical for 10 minutes to remove contamination. After the cleaning process, all samples are rinsed with deionised water (DI water) to remove the residue of Decon 90. The samples are then dipped in isopropyl alcohol (IPA) and agitated with medium ultrasonic power for 10 minutes. Finally, the samples are rinsed in DI water again and dried off with nitrogen (N_2) gas. Then, 8 PET samples are thermally annealed under different annealing temperatures for 60 min (as outlined in Table 1) in Lenton VTF tube furnace within N_2 ambient with incoming N_2 flow rate kept at 5.0 L/min throughout the annealing process. An original PET sample (without annealing) is used for comparison purpose (i.e. as a reference sample).

Table 1. Annealing conditions of PET samples (in N_2 ambient).

Sample	T ($^{\circ}\text{C}$)	t (min)	Remarks
1	Original	Original	Original (not annealed)
2	80	60	Annealed at different temperatures for 60 min
3	100	60	
4	120	60	
5	140	60	
6	160	60	
7	180	60	
8	200	60	
9	220	60	

After annealing, thermal properties of the samples (including the original sample) are characterised by Perkin-Elmer Pyris 1 differential scanning calorimeter (DSC). In this test, the samples are heated in N_2 atmosphere from 0°C to 300°C at $20^{\circ}\text{C}/\text{min}$ (first heating), held for 1 minute at 300°C and then cooled down back to 0°C at $100^{\circ}\text{C}/\text{min}$. The samples are then heated again from 0°C to 300°C at $20^{\circ}\text{C}/\text{min}$ (second heating). The resulting DSC thermograms (where temperatures and heat flows are

measured) are extracted and analysed. From the thermograms, enthalpy of fusion (ΔH_f) of each sample is determined. From the enthalpy of fusion, corresponding sample crystallinity (X_c) is calculated by using the following equation [7]:

$$X_c (\%) = \frac{\Delta H_f}{\Delta H_{f0}} \times 100\% \quad (1)$$

where;

X_c = degree of crystallinity (%)

ΔH_f = enthalpy of fusion of the sample measured at the melting point (area under melting endotherm peak, in J/g)

ΔH_{f0} = enthalpy of fusion of 100% crystalline PET measured at the equilibrium melting point (in J/g). The value of ΔH_{f0} is quoted as 166.5 J/g from Y. Kong and J. N. Hay [7, 8].

Finally, optical transmissions of the annealed samples (including the original sample) are characterised by UV-Vis Hitachi U-2000 spectrophotometer system within the spectral range of 200 – 1100 nm.

3. Results and discussion

Table 2 summarises the results extracted from DSC measurements. The enthalpy of fusion (ΔH_f) of the sample measured at the melting point (area under melting endotherm peak) is shown together with the calculated crystallinity (X_c). From the table, it is shown that the original PET sample used in this investigation is semi-crystalline in nature with X_c equals to 25.094%. This indicates the presence of a two-phase (mixed) morphology of ordered and disordered regions within the original PET sample [9].

Table 2. Summary of enthalpy of fusion (ΔH_f) and crystallinity (X_c) of each sample extracted from DSC thermogram.

Sample	T ($^{\circ}\text{C}$)	t (min)	Enthalpy of Fusion, ΔH_f (J/g)	Crystallinity $X_c = (\Delta H_f/\Delta H_{f0})\%$
1	Original	Original	41.781	25.094
2	80	60	42.547	25.554
3	100	60	44.738	26.870
4	120	60	44.745	26.874
5	140	60	45.121	27.100
6	160	60	46.616	27.998
7	180	60	46.760	28.084
8	200	60	47.256	28.382
9	220	60	47.836	28.730

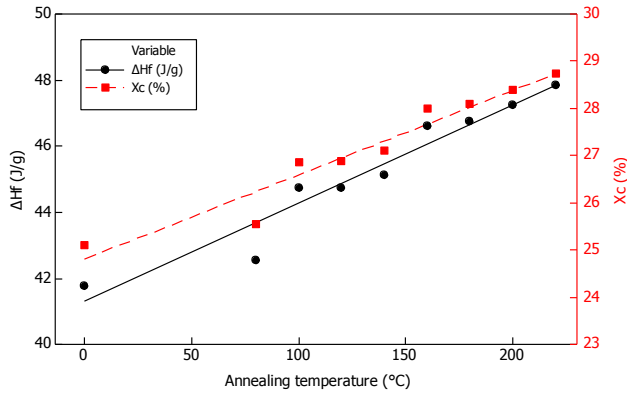


Fig. 2. Plot of ΔH_f and X_c of samples with increased annealing temperature ($t = 60$ min).

Fig. 2 shows a plot of ΔH_f and X_c of samples with increased annealing temperature ($t = 60$ min). From the figure, it can be seen that the measured enthalpy of fusion (ΔH_f , on primary y-axis) increases with increased annealing temperature. The increased enthalpy of fusion results in increased sample's crystallinity (X_c , on secondary y-axis) as calculated from equation (1). The increase in X_c is believed to be due to PET molecules gain more kinetic energy that gives them more flexibility to move around and arrange themselves into a more ordered chain segments thus forming higher density of crystalline regions within the samples at higher annealing temperatures [10, 11].

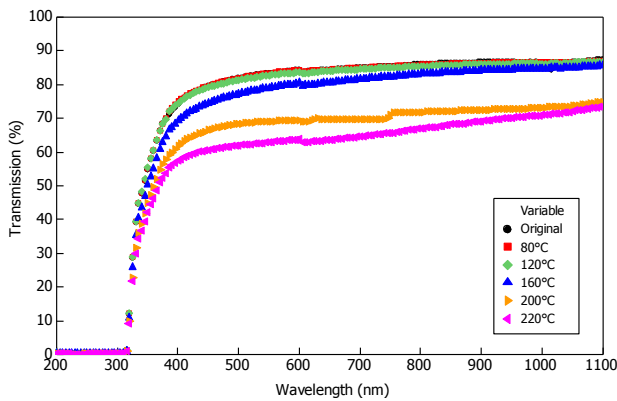


Fig. 3. Optical transmissions of samples with increased annealing temperature ($t = 60$ min) within spectral region of 200 – 1100 nm.

Fig. 3 shows the optical transmission of samples with increased annealing temperature ($t = 60$ min) within spectral wavelength of 200 – 1100 nm. The original PET sample is also plotted in the graph for comparison purpose. From this figure, it is clearly shown that the original PET has a very high optical transmission (around 85%) in the visible and extended into IR region, making it suitable as a superstrate material in thin film silicon solar cells which typically absorb the incident light until 1100 nm (for crystalline-based silicon cells) [12]. It is also evident that as annealing temperature increases, optical transmission

decreases. The minimum transmission of around 65% (average in the visible and IR regions) is recorded at the maximum annealing temperature; 220°C. The reduced transmission is believed to be due to scattering effects of the incident light by various sizes of growing crystallites within the annealed PET samples [13]. At low annealing temperature, nucleation is only about to start. The crystallites are very small in their sizes and they scatter only small amount of the incident light. As the annealing temperature increases, multiple nucleation centres being formed. Crystal growth takes place very significantly within the samples. Crystallites grow bigger with increasing temperature leading to formation of higher volume fraction of crystallites [14]. This increases the X_c of the samples (as previously shown in Fig. 2) and causes the light scattering to be more pronounced causing a more profound reduction in optical transmission [15].

Fig. 4 plots the correlation between the optical transmission and crystallinity (X_c) of the annealed PET samples at wavelength of 500, 700 and 1100 nm (i.e. different photon energies). These 4 regions are illustrated to signify regions with strong solar irradiance (W/m^2) from solar spectrum [16] and where typical thin film silicon solar cells are designed to operate [17]. From the graph, it can be seen that as X_c of the sample increases, the optical transmission reduces gradually until a sharp reduction at X_c of more than 28% (i.e. at temperature $\geq 180^\circ C$, with 60 min annealing).

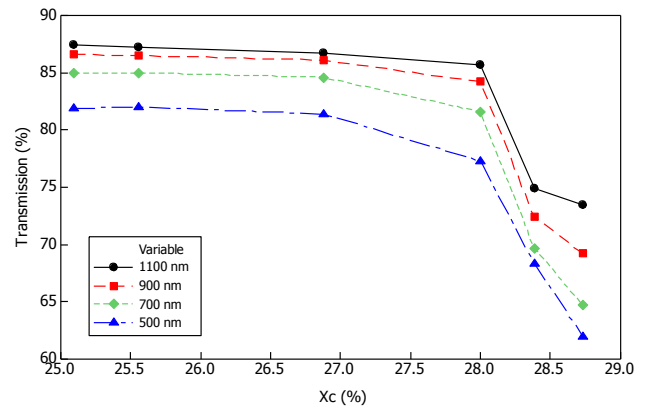


Fig. 4. Relationship between optical transmission and crystallinity of samples with increased annealed temperature ($t = 60$ min).

Besides, the graph also shows that the wavelength of 1100 nm (in IR region) possesses the highest optical transmission with increasing crystallinity compared to the other wavelengths. This is very desirable in the fabrication of superstrate thin film silicon solar cells since the incident light in the IR region with photon energy of more than 1.12 eV will be strongly absorbed by the silicon layer for photogeneration process [18]. However, moderate annealing temperature or time normally produces moderate device performance due to small grain size and low film quality of the silicon absorber layer [19]. Small grain size implies higher density of grain boundaries within the film that impede carrier flow by promoting more recombination. Low film quality means more defects

due to imperfect crystal formation, hence higher number of available carrier trap centres. Both features tremendously reduce diffusion length of the carriers and are known to be very detrimental to the solar cells performance [20].

On the contrary, a very high annealing temperature or prolonged time normally increases the grain size and improves the film quality significantly but simultaneously produces PET superstrate with low optical transmission values due to more intense light scattering events. This issue places a big constraint and demands delicate optimisations of the annealing parameters during the solar cells development. On the other hand, these effects are not critical for thin film silicon solar cells in substrate-configuration since the substrate is used merely as a device carrier (beneath below the device), not a window to the incident sunlight [21]. So, the effects discussed above can be omitted.

4. Conclusions

In this paper, thermal annealing and optical transmission of PET plastic for applications in thin film silicon solar cells in superstrate orientation are studied. DSC measurement shows that the original PET sample is semi-crystalline in nature with X_c of 25.094%. Plot of ΔH_f and X_c of samples with increased annealing temperature ($t = 60$ min) illustrates that both parameters increase almost linearly with increased annealing temperature. Optical transmission measurement reveals that the original PET has a very high optical transmission (around 85%) in the visible IR region, making it suitable as a superstrate material in thin film silicon solar cells. However, the transmission decreases with increased annealing temperature and is believed to be due to scattering effects of the incident light by various sizes of growing crystallites within the annealed samples. Correlation plot between the optical transmission and crystallinity (X_c) of the annealed samples shows that as X_c increases, the optical transmission reduces gradually until a sharp reduction at X_c of more than 28% (i.e. at temperature $\geq 180^\circ\text{C}$). These effects are very critical in the fabrication of thin film silicon solar cells in superstrate orientation but pose no issues for substrate orientation.

Acknowledgements

The support of Universiti Sains Malaysia and financial assistance from Incentive Grant 1001/PFIZIK/821061 is gratefully acknowledged. Thanks to Penfibre Sdn. Bhd. (Film Division, Malaysia) for contributing the PET samples for this work.

References

- [1] J. K. Rath, Y. Liu, A. Borreman, E. A. G. Hamers, R. Schlatmann, G. J. Jongerden, R. E. I. Schropp, *Journal of Non-Crystalline Solids* **354**, 2381 (2008).
- [2] Y. Kishi, H. Inoue, K. Murata, S. Kouzuma, M. Morizane, H. Shibuya, H. Nishiwaki, Y. Kuwano, *Jpn. J. Appl. Phys.* **31**, 12 (1992).
- [3] A. W. Blakers, T. Armour, *Solar Energy Materials & Solar Cells* **93**, 1440 (2009).
- [4] A. V. Shah, H. Schade, M. Vanecek, J. Meier, E. Vallat-Sauvain, N. Wyrsh, U. Kroll, C. Droz, J. Bailat, *Prog. Photovolt: Res. Appl.* **12**, 113 (2004).
- [5] R. Brendel, *Thin-Film Crystalline Silicon Solar Cells: Physics and Technology*, Wiley-VCH, 2001.
- [6] M. Z. Pakhuruddin, K. Ibrahim, A. Abdul Aziz, *International Journal of Polymeric Materials and Polymeric Biomaterials* **61**, 669 (2012).
- [7] Y. Kong, J. N. Hay, *Polymer* **44**, 623 (2003).
- [8] Y. Kong, J. N. Hay, *Polymer* **43**, 3873 (2002).
- [9] J. Hadac, P. Slobodian, P. Saha, *Journal of Materials Science* **42**, 3724 (2007).
- [10] Ruey-Shi Tsai, Da-Kong Lee, Han-Yu Fang, Hong-Bing Tsai, *Asia-Pac. J. Chem. Eng.* **4**, 140 (2009).
- [11] G. Ellis, F. Roman, C. Marco, M. A. Gomez, J. G. Fatou, *Spectrochimica Acta Part A* **51**, 2139 (1995).
- [12] M. A. Green, K. Emery, D. L. King, S. Igari, W. Warta, *Prog. Photovolt: Res. Appl.* **9**, 287 (2001).
- [13] E. Ashford, M. A. Bachmann, D. P. Jones, D. H. Mackerron, *Trans IchemE* **78**, Part A, 2000.
- [14] R. C. Roberts, *Polymer* **10**, 117 (1969).
- [15] H. Ouyang, W. H. Lee, M. C. Shih, *Macromolecules* **35**, 8428 (2002).
- [16] J. Nelson, *The Physics of Solar Cells*, Imperial College Press, 2003.
- [17] M. A. Green, *Silicon Solar Cells: Advanced Principles and Practice*, Centre for Photovoltaic Engineering, 1995.
- [18] M. A. Green, *Solar Cells Operating Principles, Technology and System Applications*, Prentice Hall, 1982.
- [19] P. Pathi, Ö. Tüzün, A. Slaoui, *Mater. Res. Soc. Symp. Proc.*, 1153 (2009).
- [20] T. Dylla, S. Reynolds, R. Carius, F. Finger, *Journal of Non-Crystalline Solids* **352**, 1093 (2006).
- [21] M. Ito, K. Ro, S. Yoneyama, Y. Ito, H. Uyama, T. Mates, M. Ledinsky, K. Luterova, P. Fojtik, H. Stuchlikova, A. Fejfar, J. Kocka, *Thin Solid Films* **442**, 163 (2003).

*Corresponding author: zamirlitho@gmail.com